JOURNAL OF BACTERIOLOGY, Aug. 1997, p. 5062–5071 Vol. 179, No. 16
0021-9193/97/$04.00+0

Characterization of a Transposon Tn*916*-Generated Mutant of *Haemophilus ducreyi* 35000 Defective in Lipooligosaccharide Biosynthesis

BRADFORD W. GIBSON,[1] ANTHONY A. CAMPAGNARI,[2] WILLIAM MELAUGH,[1] NANCY J. PHILLIPS,[1] MICHAEL A. APICELLA,[3] SUSAN GRASS,[4] JING WANG,[5] KATHERINE L. PALMER,[4] AND ROBERT S. MUNSON, JR.[5]*

Department of Pharmaceutical Chemistry, University of California, San Francisco, California 94143-0446[1]; Departments of Medicine and Microbiology, State University of New York at Buffalo, Buffalo, New York 14214[2]; Department of Microbiology, University of Iowa, Iowa City, Iowa 52242[3]; Department of Pediatrics, Washington University School of Medicine, St. Louis, Missouri 63110[4]; and Children's Hospital Research Foundation, Department of Pediatrics, and Department of Medical Microbiology and Immunology, The Ohio State University, Columbus, Ohio 43205[5]

Received 6 January 1997/Accepted 5 June 1997

To define the role of the surface lipooligosaccharide (LOS) of *Haemophilus ducreyi* in the pathogenesis of chancroid, Tn*916* mutants of *H. ducreyi* 35000 defective in expression of the murine monoclonal antibody (MAb) 3F11 epitope on *H. ducreyi* LOS were identified by immunologic screening. One mutant, designated 1381, has an LOS which lacks the MAb 3F11 epitope and migrates with an increased mobility on sodium dodecyl sulfate-polyacrylamide gel electrophoresis. The gene disrupted by the Tn*916* element in strain 1381 was identified by cloning the sequences flanking the Tn*916* element. The sequences were then used to probe a λDASHII genomic library. In strain 1381, Tn*916* interrupts a gene which encodes an open reading frame (ORF) with an M_r of 40,246. This ORF has homology to the product of the *rfaK* gene of *Escherichia coli*. The major LOS glycoform produced by strain 1381 was analyzed by using a combination of mass spectrometry, linkage and composition analysis, and ^{1}H nuclear magnetic resonance spectroscopy. The major LOS species was found to terminate in a single glucose attached to the heptose (L-*glycero*-D-*manno*-heptose, or Hep) trisaccharide core. In the wild-type strain 35000, glucose serves as the acceptor for the addition of the D-*glycero*-D-*manno*-heptose (or DDHep), which extends to form the mature branch of the *H. ducreyi* LOS. This mature oligosaccharide is in turn partially capped by the addition of sialic acid (NeuAc), i.e., NeuAc2α→3Galβ1→4GlcNAcβ1→3Galβ1→4DDHepα1→6Glcβ1 (W. Melaugh et al., Biochemistry 33:13070–13078, 1994). Since this LOS terminates prior to the addition of the branch DD-heptose, this gene is likely to encode the D-*glycero*-D-*manno*-heptosyltransferase. Strain 1381 exhibits a significant reduction in adherence to and invasion of primary human keratinocytes. This defect was complemented by the cloned heptosyltransferase gene, indicating that the terminal portion of the LOS oligosaccharide plays an important role in adherence to human keratinocytes.

Haemophilus ducreyi is one of the causative agents of genital ulcer disease, which is prevalent in many developing countries (1, 30, 43). More importantly, it has been shown that *H. ducreyi* infection facilitates the heterosexual transmission of the human immunodeficiency virus (HIV), particularly in geographic areas where both diseases are prominent (16, 19, 53, 58). Because of the association between *H. ducreyi* infection and HIV transmission, the identification of specific bacterial factors which contribute to the pathogenesis of chancroid is important. Although the mechanisms of virulence are not well understood, putative virulence determinants have recently been identified and characterized. In 1992, Alfa reported that *H. ducreyi* produced a cell-associated cytotoxin (2). This cytotoxin has now been identified as a homolog of the hemolysins produced by *Serratia marcescens* and *Proteus mirabilis* (32, 54). Mutants deficient in cytotoxin expression have been generated; these mutants fail to kill human foreskin fibroblasts in culture (4, 31). Purven and Largergard identified a secreted toxin which kills epithelial cells (40). This toxin has recently been identified as a homolog of the cytolethal distending toxin previously reported to be produced by *Campylobacter jejuni* and certain *Escherichia coli* strains (11).

The lipooligosaccharides (LOS) of *H. ducreyi* have also been implicated as important virulence factors. Several studies have demonstrated that *H. ducreyi* LOS cause ulcers in rabbits and mice (9, 21, 55). Recent structural studies have begun to define the LOS glycoforms expressed by several different *H. ducreyi* strains, including strains 35000, ITM5535, ITM3147, and ACY1 (27, 29, 45). In addition, recent data have demonstrated that the principal LOS glycoform expressed by most *H. ducreyi* strains is highly sialylated on the terminal galactose residue of *N*-acetyllactosamine in a manner similar to that previously reported for *Neisseria gonorrhoeae* (27; reviewed in reference 39). A recent in vitro study used extremely high concentrations of LOS isolated from strain 35000 to inhibit the adherence of these bacteria to human foreskin fibroblasts, indirectly suggesting a role of the LOS in adherence (3).

To better understand the role of LOS in the pathogenesis of chancroid, we have begun to characterize defined mutations in the biosynthetic pathway for *H. ducreyi* LOS (8). In this report, we have characterized a Tn*916* mutant of strain 35000 which produces an LOS which lacks DD-heptose and the subsequent sugar residues distal to this heptose. This LOS mutant exhibits a markedly reduced ability to adhere to human keratinocytes compared to the parent strain. These data directly implicate

* Corresponding author. Mailing address: Children's Hospital Research Foundation, 700 Children's Dr., Columbus, OH 43205. Phone: (614) 722-2735. Fax: (614) 722-3273. E-mail: rmunson@chi.osu.edu.

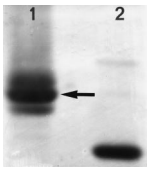

FIG. 1. Silver-stained SDS-polyacrylamide gel of LOS preparations from *H. ducreyi* 35000 (lane 1) and 1381 (lane 2). The murine MAb 3F11 binding glycoform is marked with the arrow.

the terminal oligosaccharide region of *H. ducreyi* LOS as an important ligand in attachment to human keratinocytes, which are most likely the first cell type encountered by the bacterium during the early stages of infection.

MATERIALS AND METHODS

Materials. Sodium borodeuteride (98% D) and 2,5-dihydroxybenzoic acid were purchased from Aldrich (Milwaukee, Wis.). Acetonitrile, water, and methanol were obtained from Burdick and Jackson (Muskegon, Mich.). Acetic anhydride was purchased from Supelco (Bellefonte, Pa.), and methyliodide was obtained from Fluka (Switzerland). All other reagents and solvents used were of reagent grade.

Bacterial strains and culture conditions. *H. ducreyi* 35000 was grown at 35°C with 5% CO_2 on chocolate agar (Becton Dickinson). Chocolate agar plates which were supplemented with antibiotics were prepared with BBL GCII agar base, IsoVitaleX, and hemoglobin according to the manufacturer's instructions. Plates were supplemented with tetracycline at 5 μg/ml or kanamycin at 10 μg/ml as appropriate. *E. coli* strains were grown in Luria-Bertani (LB) plates or in LB broth supplemented with antibiotics as appropriate.

Recombinant DNA methods. Standard recombinant DNA methods were used as described previously (24, 48) or as specified by the manufacturers. The construction of the λDASHII genomic library was described previously (32). The shuttle vector pLS88 was described by Willson et al. (59), and the pSC101-based vector pWKS30 was constructed by Wang and Kushner (57). Plasmids pSuperCos I and pCRII were obtained from Stratagene (La Jolla, Calif.) and Invitrogen (San Diego, Calif.), respectively. Tn*916* mutagenesis was performed by using pAM120 as described previously (32). DNA sequence was determined in both directions, using Sequenase (U.S. Biochemical Corp.) according to the manufacturer's directions. Contig assembly and sequence analysis were performed with the Lasergene software (DNASTAR, Madison, Wis.). Homology determinations and sequence alignment were performed with the NCBI BLAST server and with the GAP program from the Wisconsin sequence analysis package (Genetics Computer Group, Madison, Wis.).

Preparation and analysis of LOS. LOS from each *H. ducreyi* strain was prepared by a modification of the microphenol method previously described (9). The LOS preparations were analyzed by sodium dodecyl sulfate (SDS)-polyacrylamide gel electrophoresis (PAGE) on a 14% acrylamide gel as previously reported (9).

Immunologic screening. Screening for LOS mutants in the *H. ducreyi* Tn*916* library was performed by using a colony lift assay. Ten 150- by 15-mm chocolate plates containing approximately 10,000 tetracycline-resistant *H. ducreyi* colonies were screened. Colonies were lifted from 24-h-old plates onto nitrocellulose filters, which were then blocked with 3% bovine serum albumin. The culture plates were returned to the incubator to allow the colonies to regrow. The filters were incubated for 1 h with monoclonal antibody (MAb) 3B9, which recognizes a surface-exposed epitope on a 18-kDa outer membrane protein of *H. ducreyi* (49). This epitope phase varies at a rate of less than $1:10^4$ colonies. MAb 3B9 bound to the colonies was detected with a goat anti-mouse immunoglobulin G-phosphatase conjugate (Kirkegaard & Perry, Gaithersburg, Md.). The filter was developed with fast red TR/naphthol AS-MX (Sigma Chemical Company, St. Louis, Mo.). The same filters were washed in Tris-buffered saline (50 mM Tris, 100 mM NaCl [pH 7.0]) and then incubated overnight with MAb 3F11. 3F11 binding to the colonies was detected by using a goat anti-mouse immunoglobulin M-peroxidase conjugate (Kirkegaard & Perry). The filters were developed with horseradish peroxidase reagent (Bio-Rad, Richmond, Calif.). The filters were washed in Tris-buffered saline after color development was completed. Colonies which bound both 3B9 and 3F11 stained purple, while those which bound only 3B9 stained red. Survey of the 10 filters revealed seven colonies which bound only MAb 3B9.

Preparation of LOS and LOS-derived oligosaccharides. LOS was prepared from *H. ducreyi* 35000 and 1381 by using a phenol-water extraction procedure as described by Apicella et al. (5). LOS was O-deacylated by treatment with hydrazine under mild conditions (37°C, 30 min) followed by precipitation with chilled acetone. An oligosaccharide fraction was generated from approximately 1 mg of intact LOS by mild acid hydrolysis in 1% acetic acid for 2 h at 100°C. The released oligosaccharide pool was then separated from the largely insoluble lipid A by centrifugation (5,000 × *g*, 20 min at 4°C) and lyophilized. The lyophilized oligosaccharide pool was further purified and desalted by gel filtration chromatography on a Bio-Rad SEC column, with the eluent monitored by refractive index. The single broad peak obtained from the strain 1381 preparation was pooled and lyophilized. Details of all these procedures have been published elsewhere (29, 36).

Composition and methylation analysis. To determine the composition and linkages of the individual sugars in the mutant LOS, the oligosaccharide pool was first analyzed for monosaccharides after hydrolysis in 2 M trifluoroacetic acid for 3 h at 100°C. The hydrolysates were evaporated to dryness, redissolved in 20 μl of H_2O, and dried. Monosaccharide separation and quantitation were carried out by high-pH anion-exchange chromatography with pulsed amperometric detection (36). For linkage analysis, approximately 50 μg of the total oligosaccharide fraction was subjected to permethylation, using a modification of the technique of Levery and Hakomori (23). The partially methylated alditol acetates were analyzed by gas chromatography (GC)-mass spectrometry (MS) using a VG70SE mass spectrometer equipped with a Hewlett-Packard 5890 gas chromatograph equipped with a 30-m DB-1 column (J&W Scientific).

MS. To determine the molecular masses and compositions of LOS from strain 1381, the acid-released oligosaccharide pool and O-deacylated LOS were analyzed by liquid secondary ion MS (LSIMS), electrospray ionization (ESI)-MS, and matrix-assisted laser desorption ionization (MALDI). These methods as applied to the analysis of LOS have been described in detail elsewhere (12, 13, 28). For LSIMS analysis, a thioglycerol-glycerol (1/2, vol/vol) matrix was used, and samples were mass analyzed on a Kratos MS 50S mass spectrometer (Kratos, Manchester, England). A primary ion beam of 10 keV was used to ionize the samples, and secondary ions were accelerated at 6 kV. Scans were acquired at 300 s/decade and recorded on a Gould electrostatic recorder. Ultramark 1206 was used for manual calibration to an accuracy better than ±0.2 Da. For ESI-MS analysis, a Platform quadrupole mass spectrometer (MicroMass, Manchester, England) in the negative-ion mode was used. Samples were first dissolved in water and then injected (3-μl aliquot, ≈5 μg) via a Rheodyne injector into a constant stream of H_2O-CH_3CN (3/1, vol/vol) containing 1% acetic acid running at 3 to 4 μl/min. Mass calibration was carried out with an external cesium nitrate reference, using the supplied commercial software. For MALDI analysis of O-deacylated LOS, ca. 0.2 μg of sample was dissolved in 1 to 2 μl of acetonitrile-water and mixed with an equal volume of 100 mM 2,5-dihydroxybenzoin acid. One microliter of this sample-matrix solution was dried on the MALDI probe at room temperature and analyzed with a PerSeptive Biosystems (Framingham, Mass.) Voyager MALDI time-of-flight (MALDI-TOF) mass spectrometer equipped with a nitrogen laser (337 nm) and run in the negative-ion mode with delayed extraction (56). The resulting spectra were calibrated with an external reference consisting of the peptides angiotensin (M_r = 1,296.5) and adrenocorticotropin (M_r = 2,465.7).

NMR analysis. ^1H nuclear magnetic resonance (NMR) analyses of the high-pressure liquid chromatography-purified oligosaccharide fraction from strain 1381 were carried out to determine the anomeric configurations of the sugars

TABLE 1. Composition and methylation analysis of strain 35000 and strain 1381 oligosaccharides

Strain	Composition analysis[a] (molar ratio relative to glucose)					Methylation analysis[d] (relative peak area)							
	Galactose	Glucose	L,D-Heptose	D,D-Heptose[b]	$GlcNH_2$	t-Gal	3-Gal	x-Glc[e]	t-Hep	2-Hep	3,4-Hep	4-Hep	4-GlcNAc
35000	2.5	1.0	2.7	0.8	1.1	1.0	1.5	1.7	0.7	0.9	0.7	0.6	1.8
1381		1.0	2.3[c]					1.0	1.1	0.5	0.5		

[a] Composition and methylation data for the parental strain 35000 have been previously published (28) and are reported here for comparative purposes only.
[b] This second heptose has been identified as D-*glycero*-D-*manno*-heptose, as opposed to the major core heptoses, which are L-*glycero*-D-*manno*-heptoses.
[c] The lower than expected relative molar ratios for heptose compared to glucose are partially explained by background contamination of glucose.
[d] Partially methylated alditol acetates are abbreviated according to their substitution pattern as follows: t-Gal is 1,5-di-*O*-acetyl-2,3,4,6-tetra-*O*-methylgalactitol, 3-Gal is 1,3,5-tri-*O*-acetyl-2,4,6-tri-*O*-methylgalactitol, etc.
[e] 6-Glc was observed in strain 35000, and terminal glucose (t-Glc) was observed in strain 1381.

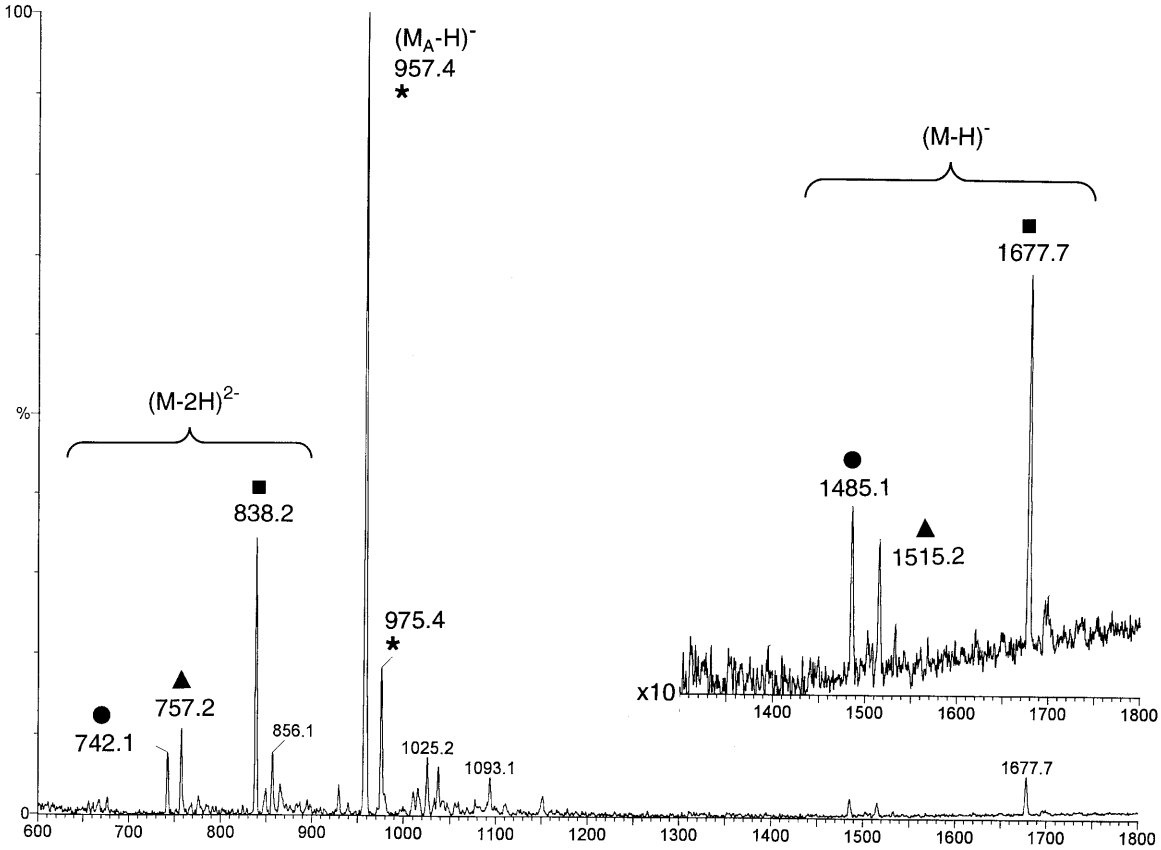

FIG. 2. Negative-ion ESI-MS spectrum of acid-cleaved oligosaccharide fraction of *H. ducreyi* 1381 LOS. The peaks associated with the major oligosaccharide are labeled with asterisks and are observed as two single charged species at $(M - H)^-$ = 957.4 and $(M - H + H_2O)^-$ = 975.4 with an average mass of 958.4 Da. Note the small amount of wild-type oligosaccharide peaks with M_rs of 1,678.7 (*m/z* 838.2 and 1,677.7; ■) and 1,516.4 (*m/z* 757.2 and 1,515.2; ▲) corresponding to doubly and singly charged species. Also observed is a fourth component with an M_r of 1,486.2 (*m/z* 742.1 and 1,485.1; ●) that would nominally correspond to an oligosaccharide containing one less heptose (ΔM = 192.2 Da) than the 1678.7-M_r oligosaccharide. See text and Table 2 for details.

and to confirm the linkage assignments. For these experiments, approximately 100 μg of oligosaccharide was analyzed on a GE GN-500 MHz NMR apparatus under conditions identical to those originally reported for the NMR characterization of the major oligosaccharide from the parent strain, *H. ducreyi* 35000 (29).

Adherence and invasion of human keratinocytes. The isolation of human keratinocytes and preparation of monolayers have been described elsewhere (7). In addition, we used the standard adherence assay conditions, including the preparation of bacterial inocula, described by Brentjens et al. (7). *H. ducreyi* invasion of keratinocytes was assessed by using the gentamicin protection assay described by St. Geme and Falkow (52). Briefly, the standard adherence assay was performed in duplicate plates as described previously (7). One plate was processed to measure adherence, and gentamicin sulfate (35 μg/ml) was added

TABLE 2. ESI-MS analyses of *O*-deacylated LOS and oligosaccharides from strain 1381[a]

Sugars	Form	M_r		Relative abundance (%)	Proposed composition
		Observed[b]	Calculated		
O-deacylated LOS	A′	1,974.0	1,973.8	94	Hex Hep_3 Kdo(P) lipid A[c]; $-H_2O$
	A	1,991.0	1,991.8	80	**Hex Hep_3 Kdo(P) lipid A**
	A″	2,006.0		72	Hex Hep_3 Kdo(P) lipid A; +14 Da
	B′	2,097.2	2,096.8	100	Hex Hep_3 Kdo(P) PEA lipid A; $-H_2O$
	B	2,115.4	2,114.8	98	**Hex Hep_3 Kdo(P) PEA lipid A**
	B″	2,130.0		81	Hex Hep_3 Kdo(P) PEA lipid A; +14 Da
Oligosaccharides	**A**	958.4	958.8	100	**Hex Hep_3 anhydro-Kdo**
	A	1,486.2	1,486.3	9	Hex_3 HexNAc Hep_3 anhydro-Kdo
	A	1,516.4	1,516.3	13	Hex_2 HexNAc Hep_4 anhydro-Kdo
	A	1,678.7	1,678.5	28	Hex_3 HexNAc Hep_4 anhydro-Kdo

[a] The major unmodified O-deacylated LOS glycoforms are indicated by the boldface type.

[b] All molecular weights for O-deacylated LOS are reported as average values based on both doubly and triply deprotonated charged molecular ions, $(M - 2H)^{2-}$ and $(M - 3H)^{3-}$, with the exception of the 2,130-M_r species, whose doubly charged ion was unresolved from the sodiated adduct of the 2,115-M_r LOS. For the oligosaccharides, molecular weights are based on singly and doubly charged ions, $(M - H)^-$ and $(M - 2H)^{2-}$, with the exception of the 958.4-M_r species, which yielded only a singly charged peak.

[c] After O-deacylation, the lipid A moiety is converted into diphosphoryl diacyl-lipid A containing two N-linked β-hydroxymyristic acid chains with an average M_r of 953.0. In the LOS species containing PEA, preliminary data indicate that it is attached to one of the two phosphates on lipid A.

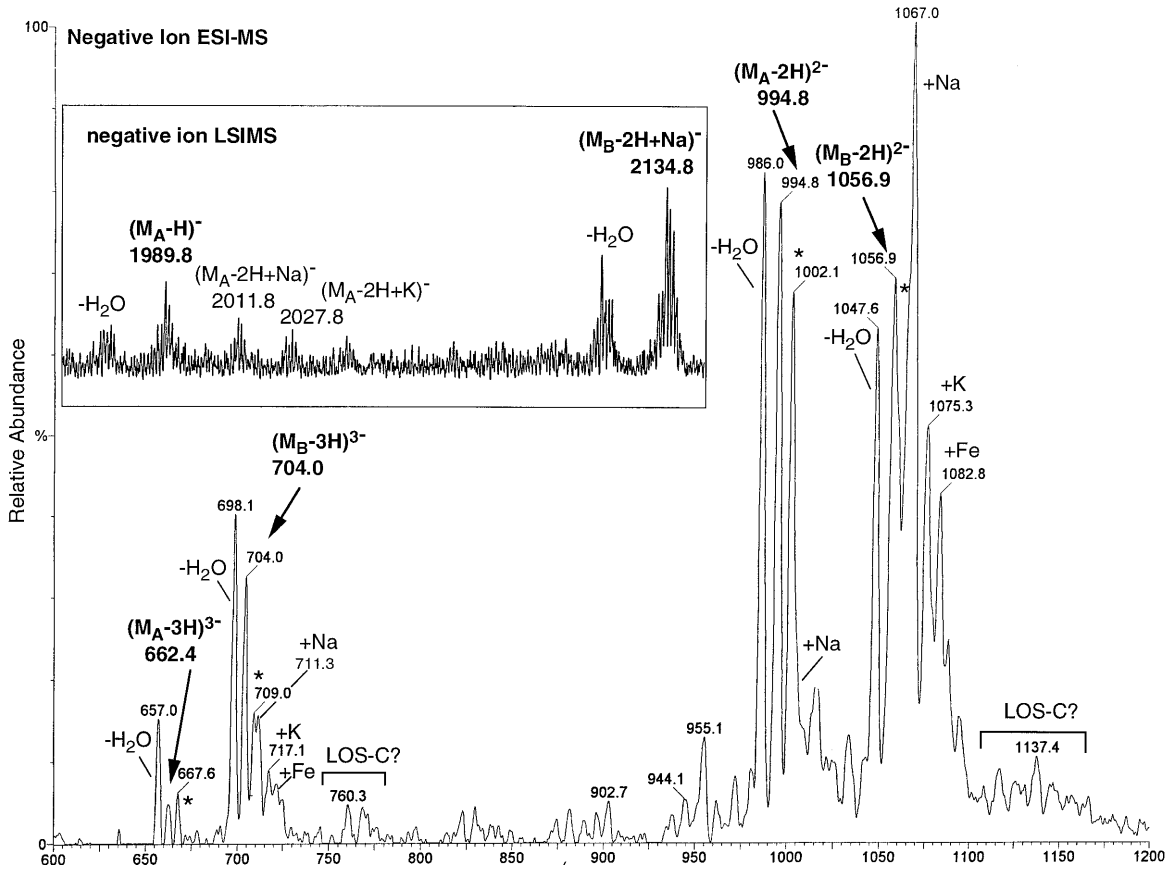

FIG. 3. Negative-ion ESI-MS spectrum of O-deacylated LOS from *H. ducreyi* 1381. The inset (top left) shows the corresponding LSIMS spectrum of the molecular ion region taken at higher resolving power. In the ESI-MS spectrum, the LOS-A and -B glycoforms have two additional peaks arising from either loss of H_2O, $(M - nH - H_2O)^{n-}$, or the addition of an unknown adduct with a mass difference of 14 to 15 Da (or 32 to 33 Da from the LOS peaks that have lost H_2O). Note that these latter peaks at *m/z* 667.6, 709.0, 1,002.1, and 1,064 (all marked by asterisks) do not appear in the LSIMS or MALDI spectra, suggesting they are artifacts of the ESI-MS experiment. The higher-mass LOS-B species contains a PEA moiety which is likely present linked to phosphate to form a phospho-PEA moiety in the lipid A region. The presence of an internal pyrophosphate linkage in the LOS species containing this additional PEA moiety accounts for the additional salt adducts in the ESI-MS spectrum, including sodium, potassium, and iron, as well as dominance of the sodiated adduct for this same species in the LSIMS spectrum. After summing the area of all related peaks for the LOS-A and LOS-B glycoforms, a ratio of 1 to 3 (A to B) is obtained. Small amount of a third LOS species (LOS-C) can be seen as subsequently confirmed in the MALDI spectrum (Fig. 4), as well as a triply charged ion for the major wild-type LOS glycoform at *m/z* 902.7. See Table 2 for the assignments of LOS composition.

to each well of the duplicate plate. This plate was allowed to incubate for an additional 2 h at 37°C. After extensive washing, the keratinocytes were lysed, and the suspension diluted and then plated out in triplicate on chocolate agar. Percent invasion was assessed by determination of CFU.

Nucleotide sequence accession number. The DNA sequence of the *losAB* region is available through GenBank (accession no. AF004712).

RESULTS

Identification of Tn*916* mutants deficient in LOS biosynthesis. A library of Tn*916* mutants was generated by electroporation of pAM120 into *H. ducreyi* 35000 as described previously (32). Seven mutants which failed to bind MAb 3F11 were characterized. A LOS preparation from each strain was analyzed by SDS-PAGE. The LOS from strain 1381 ran with the highest mobility on SDS-PAGE compared to preparations from strain 35000 and the other Tn*916* LOS mutants. A silver-stained SDS-polyacrylamide gel comparing the mobilities of the LOS from strains 35000 and 1381 is shown in Fig. 1. The LOS from strain 1381 and the mutation responsible for this phenotype were further characterized.

Structural characterization of strain 1381 LOS. For the structural characterization of LOS, a crude LOS preparation was isolated and an oligosaccharide fraction was prepared by acetic acid hydrolysis. The structure of the oligosaccharide portion of the LOS from strain 1381 was investigated by using MS, composition and linkage analysis, and ^1H NMR data. On the purified oligosaccharide fraction, composition analysis showed only two types of sugars present, heptose and glucose, in a molar ratio of 2.3 to 1 (Table 1). GC-MS of the partially permethylated alditol acetates established the presence of four sugars: a terminal glucose and terminal heptose, a 2-linked heptose, and a 3,4-linked heptose. The absence of 2-keto-3-deoxyoctulosonic acid (Kdo) was expected due to the conversion of the presumed 4-phospho-Kdo sugar to the anhydro-Kdo products during the mild-acid step (6) as reported previously for several *Haemophilus* species (34, 35, 45, 46), including the LOS from the parental *H. ducreyi* 35000 (28, 29). These reducing terminal anhydro-Kdo diastereomers are presumably destroyed during the acid hydrolysis conditions used in the monosaccharide analysis.

To determine the masses and assign a precise composition to the oligosaccharide region from the LOS of strain 1381, the acid-cleaved oligosaccharide fraction was analyzed by both LSIMS and ESI-MS after size-exclusion chromatography. The ESI-MS spectrum for the oligosaccharide fraction is shown in Fig. 2; the data are summarized in Table 2. In both cases, the

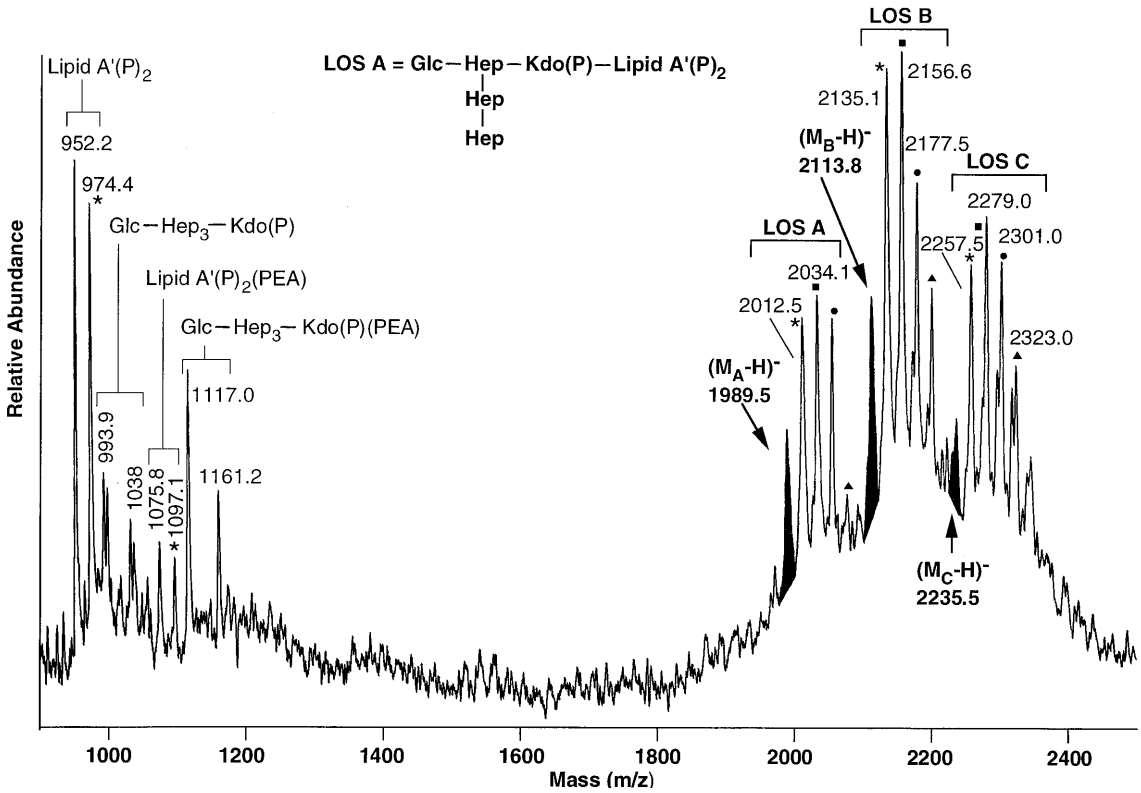

FIG. 4. Negative-ion MALDI-TOF spectrum of O-deacylated LOS from *H. ducreyi* 1381. The intact O-deacylated LOS-A, -B, and -C glycoforms are observed in their deprotonated ionic states, $(M - H)^-$, as well as several cationized states, $(M - 2H + Na)^-$ (*), $(M - 3H + 2Na)^-$ (■), $(M - 4H + 3Na)^-$ (●), and $(M - 5H + 4Na)^-$ (▲). Lipid A′$(P)_2$ refers to the diphosphorylated O-deacylated form. See Fig. 5 and the text for more details.

major peak observed corresponded to a common oligosaccharide with an isotopically resolved mass of 958.2 (LSIMS) and an average mass of 958.4 (ESI-MS). (The higher resolving power of the sector instrument under LSIMS conditions yielded isotopically resolved peaks, with the most abundant peak isotopically pure [exact mass]. The ESI-MS experiment was carried out with a quadrupole analyzer which did not resolve these isotopes and whose centroid is the average mass.) These data compare well with a calculated exact mass of 958.3 and an average mass of 958.8 for an oligosaccharide consisting of one hexose, three heptoses, and one anhydro-Kdo as expected from the composition and linkage analysis data. In addition to this major oligosaccharide peak, we observed in the ESI-MS spectrum several smaller peaks that have been previously identified as belonging to full-length wild-type oligosaccharide structures (28, 29), such as the 1679- and 1516-M_r oligosaccharide species (singly and doubly charged ions at *m/z* 1,677.7 and 838.2 and at *m/z* 1,515.2 and 757.2, respectively). These two full-length oligosaccharides correspond in mass to oligosaccharides with Galβ1-4GlcNAcβ1-3Galβ1-4DDHepα1-6Glcβ1 and GlcNAcβ1-3Galβ1-4DDHepα1-6Glc branches attached to the Hep_3-anhydro-Kdo core structure. These latter structures apparently arose from some reversion of the strain 1381 mutant back to the parental wild-type strain. Excision of the Tn*916* element is known to occur, resulting in the restoration of the parental genotype (47). A third, low-abundance oligosaccharide with a mass of 1,486 Da was also present in this oligosaccharide fraction, as evident from the presence of both singly charged and doubly charged ions at *m/z* 1,485.1 and 742.1, respectively. This oligosaccharide was not observed in our previous work on this parental strain despite it having a mass within the expected range of full-length wild-type structures (28, 29). Computer composition searches based on this experimental mass suggest that it differs from the previously determined full-length wild-type oligosaccharide (M_r = 1,678) by the absence of a single heptose residue (ΔM = 192 Da, heptose). Although this novel species could arise from the absence of a LD-heptose from the triheptose core, it is more likely that is originates from an alternative biosynthetic pathway that bypasses the addition of the branch DD-heptose. This point will be discussed later.

In contrast to the relative simplicity of the oligosaccharide MS data, analysis of the O-deacylated LOS yielded a far more complex spectrum than would have been expected from a LOS containing a single major oligosaccharide. Under ESI-MS conditions, we observed two major LOS glycoforms with average molecular weights of 1,991.6 (LOS-A) and 2,115.4 (LOS-B) (Fig. 3). Similarly, LSIMS analysis also indicated two major isotopically resolved LOS species at the same mass, although the higher-mass LOS-B was present primarily in a sodiated form (Fig. 3, inset). The lower-mass LOS-A glycoform is in excellent agreement with the oligosaccharide data after addition of the mass of diphosphoryl diacyl-lipid A moiety (ΔM = 934 Da) and correcting for the mass difference between anhydro-Kdo and phospho-Kdo, i.e., M_r average is 1,991.8 and M_r exact is 1,990.8 for the O-deacylated LOS-A species. The higher-mass peaks that belong to the second LOS-B glycoform, however, differ by the mass of phosphoethanolamine (PEA; ΔM =123 Da), a moiety not observed in MS data of the oligosaccharide fraction. In addition, a third LOS species (LOS-C) was tentatively identified as possibly containing two PEA

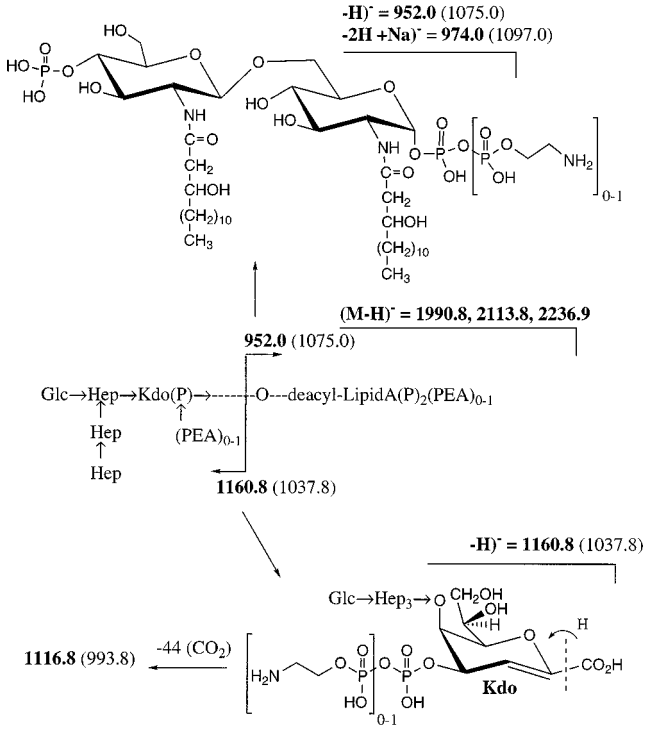

FIG. 5. Structures and masses of the molecular ions and fragments predicted from the negative-ion MALDI spectrum of O-deacylated LOS. See Fig. 4 for the experimentally determined masses. The position of the variable PEA on lipid A has not been determined.

moieties, but their precise masses could not be unambiguously assigned due to extensive salt adducts and low ion abundance.

To examine the source of the PEA substitution(s) and confirm the presence of the third LOS species (LOS-C), this same O-deacylated LOS preparation was analyzed by MALDI-TOF MS. When the LOS was analyzed by MALDI, we previously reported that masses are observed for both the intact LOS glycoforms as well as fragments arising from the oligosaccharide and lipid A moieties (12). As shown in Fig. 4, MALDI data obtained from this LOS preparation revealed three LOS glycoforms, LOS-A, -B, and -C, with molecular weights of 1,990.5, 2,114.8, and 2,236.5. The masses of LOS-A and -B were consistent with those previously observed by LSIMS and ESI-MS. The third glycoform, LOS-C, has a mass consistent with the presence of two PEA moieties compared to LOS-A, which therefore confirms the tentative assignment made from the ESI-MS spectrum (Fig. 3). In addition, fragments originating from these LOS species through glycosidic bond cleavage were identified at *m/z* 1,161 and 1,117. This latter finding is consistent with an oligosaccharide fragment having a composition of $GlcHep_3Kdo(P)PEA$ [Kdo(P) is phospho-Kdo], where the lower-mass fragment has lost CO_2 from Kdo through a subsequent fragmentation process (−44 Da) (Fig. 5). Two analogous oligosaccharide fragments that do not have this PEA moiety are also present but are only about half as abundant (see peaks at *m/z* 1,038 and 994). These oligosaccharide fragments, therefore, clearly show that the majority of the LOS-derived oligosaccharides contain one PEA moiety. Moreover, unlike oligosaccharide fragments that have an unsubstituted phosphate group on the Kdo (4′-phospho-Kdo), the PEA-containing oligosaccharide species do not undergo loss of phosphoric acid ($-H_3PO_4$), a MALDI fragmentation pathway common to most LOS-derived oligosaccharide fragments containing an unsubstituted phosphate (12). The absence of the loss of phosphoric acid suggests that it is the phosphate of phospho-Kdo that is substituted with PEA. Substitution of phosphate by PEA at this position would also explain the absence of PEA in the acid-cleaved oligosaccharide fraction as observed in the ESI-MS spectrum (Fig. 2). If PEA were substituted on the phosphate of phospho-Kdo, acid-catalyzed β-elimination of phosphate to form anhydro-Kdo would eliminate the PEA group as well.

Similarly, partial substitution of PEA is also evident in the lipid A moiety. Examination of the lower-mass region of this same MALDI spectrum shows the base peak of *m/z* 952 (and the sodiated adduct at *m/z* 974) for the expected lipid A fragment containing two N-linked β-hydroxymyristic acid groups and two phosphates. However, a second set of peaks ~123 Da higher in mass is also present at *m/z* 1,075 and 1,097, at ~50% relative abundance, providing evidence for the partial substitution of lipid A by PEA. Therefore, based in part on the wild-type oligosaccharide structure from the parental strain 35000, these data support a major LOS structure with a single glucose attached to a $Hep_3Kdo(P)$ core where phospho-Kdo is largely (~80%) modified by PEA to form phospho-PEA and where the lipid A is partially (~33%) substituted with PEA:

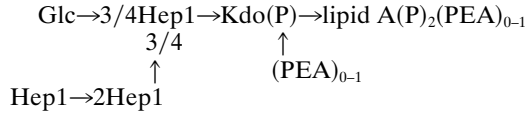

To confirm the oligosaccharide portion of the strain 1381 LOS structure and to assign linkage and anomeric configurations, proton NMR analysis was carried out on a 100-μg sample of the acetic acid-released oligosaccharide. As summarized in Fig. 6, we found anomeric proton resonances that were consistent with those previously assigned as three alpha-linked heptoses and one beta-linked glucose in the *H. ducreyi* wild-type structure (29, 46) as well as the analogous structure found in *Haemophilus influenzae* 2019 LOS (34). As described for those systems, the anomeric proton of spin system III (nonreducing terminal heptose) was least effected by the multiplicity

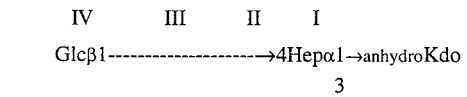

anomeric proton	δ (ppm)	*J* (Hz)
αHep I	5.099	<1
	5.079	
	5.029	
αHep II	5.703	1
	5.682	
	5.667	
αHep III	5.112	<1
βGlc IV	≈4.52*	≈7-8

FIG. 6. Anomeric proton NMR assignments of the major oligosaccharide from *H. ducreyi* 1381 (D_2O, 25°C). Shown are chemical shifts and coupling constants obtained from the one-dimensional spectrum. *, average of overlapping signals arising from reducing-terminal microheterogeneity.

TABLE 3. Oligonucleotides used in this study

No.	Sequence	Comment
1	5′CGTGAAGTATCTTCCTACAG	Tn*916* left end
2	5′GCTACTAAATTATGCGTATC CTATTCG	Used for generating probe
3	5′GGGAATTCCCCTTGCGTTTT TGGTG	5′ of *losB*, *Eco*RI site at 5′ end is underlined
4	5′GCGAGCTCCCTATTTGGGC AGTATT	3′ of *losB*, SacI site at the 5′ end is underlined

of isomers present in the reducing terminal anhydro-Kdo moiety and was seen as a single broad peak (δ 5.112, $J_{1,2}$ <1 Hz). The anomeric protons of the other two heptose spin systems, II and I, were each seen as three peaks (Fig. 6) due to their proximity to the heterogeneous reducing terminus. Based on the similarity of these peaks to the spectrum of the wild-type structure, heptoses I, II, and III were all assigned as alpha linked. The remaining high-field-shifted anomeric proton could be assigned as a beta-linked glucose and, like the heptose I and II spin systems, was perturbed by the anhydro-Kdo into three overlapping peaks (δ ≈4.52, $J_{1,2}$ ≈7 to 8). Therefore, when combined with the composition, linkage, and MS data, these NMR assignments support a pentasaccharide structure identical to that contained within the parental 35000 strain:

Glcβ1→4Hepα1→anhydro-Kdo
3
↑
Hepα1→2Hepα1

Identification of the gene interrupted by Tn*916* in strain 1381. Genomic DNA from strain 1381 was prepared, partially digested with *Sau*3A, and ligated into the cosmid vector pSuperCos I. The library was packaged in vitro and transduced into *E. coli* χ2819 (10). Clones resistant to ampicillin (plasmid marker) and tetracycline (Tn*916* marker) were identified. Plasmid DNA was prepared, and the sequence was determined from one cosmid clone by using an oligonucleotide primer which recognizes the end of Tn*916* (Table 3, oligonucleotide 1). This DNA sequence contained the end of one open reading frame (ORF) and the start of a second ORF. To clone the intact gene which had been interrupted by the Tn*916* element, an oligonucleotide complementary to the newly determined sequence was prepared (Table 3, oligonucleotide 2) and a ^{32}P-labeled PCR product was generated. The PCR product was then used to probe a λDASHII genomic library. Lambda clones were identified and plaque purified. DNA from one probe-positive λ clone with a genomic insert of 9 kb was prepared, digested with *Not*I, and ligated into the low-copy-number vector pWSK30. A number of attempts were made, without success, to clone the 9-kb genomic fragment into pWKS30. Therefore, the λ DNA was partially digested with *Sau*3A, and 4- to 9-kb fragments were ligated into *Bam*HI-digested pWSK30. The ligation mixture was transformed into *E. coli* XL1-Blue, and clones containing inserts were identified on 5-bromo-4-chloro-3-indolyl-β-D-galactopyranoside (X-Gal) plates. Clones containing the insert of interest were identified by colony hybridization using the ^{32}P-labeled PCR product as a probe. The plasmid designated pRSM1494 was further characterized.

Characterization of pRSM1494. The DNA sequence of the ORF interrupted by the Tn*916* element in strain 1381 was completely determined. This gene, designated *losB*, encodes a protein with an M_r of 40,246. The derived amino acid sequence

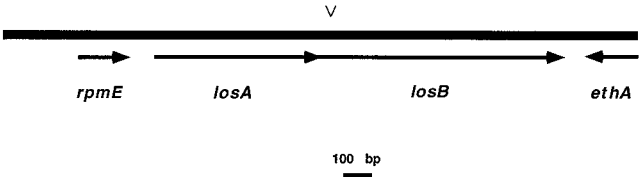

FIG. 7. Partial restriction map of pRSM1640. The sequence begins with the *Sau*3A/*Bam*HI junction of the λ clone. The positions and direction of transcription of the *rpmE*, *losA*, *losB*, and *ethA* genes are designated. The V marks the insertion of the Tn*916* element in the 1381 genomic DNA.

of the *losB* gene has homology to the product of the *E. coli rfaK* gene (24% identity and 52% similarity). The *rfaK* gene is thought to encode an *N*-acetylglucosamine glycosyltransferase (18). Immediately 5′ of the *losB* gene is a gene that we designated *losA*. The *losA* gene encodes a protein with an M_r of 25,795. The derived amino acid sequence of this gene has homology to the *lic2A* gene of *H. influenzae* (15) and the *lpsA* gene of *Pasteurella haemolytica* (38). Both of these genes are thought to encode proteins involved in LOS (or lipopolysaccharide) biosynthesis. 5′ to the *losA* gene is an ORF which encodes a peptide with an M_r of 7,917. This gene is the *H. ducreyi* homolog of the *rpmE* gene, which encodes the ribosomal protein L31. The *H. ducreyi* protein is 91% identical to the *H. influenzae* protein. 3′ to the *losB* gene is the *H. ducreyi* homolog of the *ethA* gene, which encodes exonuclease III. This gene is transcribed in the opposite direction; the stop codon is located at nucleotides 2187 to 2189. A partial map of pRSM1494 is shown in Fig. 7.

Complementation of the Tn*916* mutation in *H. ducreyi* 1381. To complement the defect in strain 1381, we attempted to clone the genomic insert from the λ clone as a *Not*I fragment into the shuttle vector pLS88 which had been modified by the addition of *Not*I restriction site (32). We were unable to clone the *Not*I fragment into pLS88 and therefore amplified the *losB* gene by PCR using oligonucleotides 3 and 4 (Table 3). The PCR product was cloned into pCRII, and then the *Eco*RI fragment containing the PCR product was cloned into *Eco*RI-digested pLS88. A clone with the appropriate restriction map was identified and designated pRSM1640. The *Eco*RI site is located immediately 3′ to the Str^r gene of pLS88, and thus the promoter for the Str^r gene may be responsible for transcription of the *losB* gene in pRSM1640. Plasmids pRSM1640 and pLS88 were transformed into strain 1381. LOS was isolated from strain 1381/pRSM1640. It had the same SDS-PAGE profile as strain 35000, indicating that the *losB* gene is sufficient to complement the mutation in strain 1381 (Fig. 8). LOS from this strain was also reactive with MAb 3F11 (data not shown).

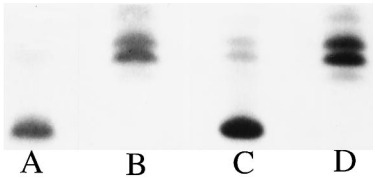

FIG. 8. Silver-stained SDS-polyacrylamide gel of LOS preparations demonstrating complementation of the mutation in strain 1381. The *losB* gene was amplified by PCR, and the amplicon was cloned into the *Eco*RI site of the shuttle vector pLS88 to form pRSM1640. LOS was isolated from each strain, subjected to SDS-PAGE, and silver stained. Lane A, LOS from strain 1381; lane B, LOS from strain 1381/pRSM1640; lane C, LOS from strain 1381/pLS88; lane D, LOS from strain 35000.

TABLE 4. Adherence to and invasion of keratinocytes by strains 35000 and 1381

Strain	% Adherence (mean ± SD)	% Invasion (mean ± SD)
35000	15 ± 1.5	7.2 ± 1.8
1381	4.5 ± 1	0.08 ± 0.05
1381/pLS88	5.3 ± 1.4	0.1 ± 0.05
1381/pRSM1640	13.3 ± 1.2	5.2 ± 1.1

Strain 1381 fails to exhibit normal adherence to and invasion of normal human keratinocytes. Mid-log-phase *H. ducreyi* cells were coincubated with human keratinocyte monolayers for 2 h. Nonadherent bacteria were removed by washing, and the number of adherent bacteria was determined as described previously (7). Under these conditions, 15% of the CFU of strain 35000 put into the coculture were adherent. In contrast, approximately 5% of strain 1381 cells were adherent. Complementation of the Tn*916* mutation in 1381 with pRSM1640 restored the adherent phenotype (Table 4). Similarly, in a gentamicin protection assay, the invasive capability of strain 35000 was abolished by the *losB* mutation in strain 1381, and the invasive phenotype was restored by complementation with pRSM1640.

DISCUSSION

Transposon Tn*916* and the related transposon Tn*1545*Δ*3* have proven to be powerful tools for the construction of mutants of *H. ducreyi*. We and others have previously identified mutants deficient in hemolysin (32, 54), hemoglobin binding protein (51), and LOS biosynthetic genes (51) by using these genetic elements. In this study, we used Tn*916* mutagenesis to identify a mutant deficient in the D-*glycero*-D-*manno*-heptose heptosyltransferase. Immunologic screening was performed with two murine MAbs of different isotypes, using different isotype-specific detection reagents. Colonies which stained red had lost the 3F11 binding specificity, while colonies which stained purple retained the 3F11 binding specificity, greatly simplifying the identification of the LOS mutants. One mutant lacking the 3F11 epitope was characterized in detail. The major glycoform of the LOS produced by this strain, designated 1381, lacked residues distal to the single glucose extending off heptose-I. In the wild-type strain, this glucose is linked to D-*glycero*-D-*manno*-heptose, which is further extended by a tri- or tetrasaccharide that contains the terminal *N*-acetyllactosamine (MAb 3F11 epitope) and sialyl-*N*-acetyllactosamine epitopes (27, 29). Therefore, the defect contained in this mutant strain 1381 precludes the normal extension of the major oligosaccharide branch through the inability to form the DD-heptosylα1-6 linkage to glucose. This defect may also explain the oligosaccharide species observed in the ESI-MS spectra of the oligosaccharide fraction with a mass of 1,486 Da. As suggested earlier, this unexpected oligosaccharide species was consistent with a full-length oligosaccharide but lacking one heptose residue compared to the major wild-type structure with a mass of 1,678 Da. Given that the defect in this mutant is associated with the inability to add the branch DD-heptose to glucose, such a species may arise from an alternative biosynthetic pathway that skips this DD-heptose and goes on to form a lacto-*N*-neotetraose branch, Galβ1→4GlcNAcβ1→3Galβ1→4Glc--. We have previously noted that the African strain 33921 is capable of bypassing the DD-heptose by forming GlcNAcβ1→3Galβ1→4Glc-- (27), as was the major LOS from a strain reported by Schweda et al. (46) that made a lactose disaccharide branch (Galβ1→4Glc--) off the conserved triheptose core.

In *Salmonella typhimurium*, the heptose biosynthetic pathway has been characterized in detail (41). In *Salmonella*, D-*glycero*-D-*manno*-heptose is thought to be the precursor of D-*glycero*-L-*manno*-heptose. Assuming that the biosynthetic pathway is conserved in *H. ducreyi*, we conclude that the mutation responsible for the phenotype of strain 1381 is in the gene encoding the D-*glycero*-D-*manno*-heptose heptosyltransferase. Our conclusion is also consistent with the weak homology observed between LosB and another glycosyltransferase, the product of the *E. coli rfaK* gene.

The amount and distribution of PEA were also determined in the LOS of strain 1381. The amount of PEA found in the LOS of this mutant was greater than that previously found in the LOS of the parental strain. In the mutant LOS, MS analysis identified two distinct sites of nonstoichiometric PEA substitution, one on the lipid A and one on the phospho-Kdo. Surprisingly, no PEA was found to be substituted off the triheptose core. Reexamination of the LOS from strain 35000 suggests that the PEA-containing glycoforms also contain PEA on phospho-Kdo (11a) but none on the lipid A or heptose, the latter of which was presumed to be the site of attachment based on the similarity in the structures of the *H. influenzae* and *H. ducreyi* LOS cores. This additional PEA substitution may underlie an adaptive mechanism for the mutant, which now has a much smaller LOS and potentially less stable outer membrane. We have recently reported on these modifications in the LOS of *H. ducreyi* and *H. influenzae* (12), as have Masoud et al. (25) in their characterization of the LOS of *H. influenzae* serotype b strain Eagan. It is interesting that substitution of phosphate on lipid A has also been found in the LOS of *S. typhimurium* (14), *Neisseria meningitidis* (20), and *Moraxella catarrhalis* (17, 26). In *S. typhimurium*, this lipid A alteration is the result of a mutation in a two-component regulatory system which is thought to play a role in virulence (42).

Recent studies have demonstrated that *H. ducreyi* can adhere to and invade some eucaryotic cell lines. However, the actual mechanism and the bacterial components involved in this activity have not been defined. In 1993, Lagergard and coworkers noted that *H. ducreyi* cells could withstand treatment at 56°C for 30 min without losing the ability to adhere to HEp-2 cells (22). Some binding was observed after treatment of the *H. ducreyi* cells at 100°C for 30 min. This finding implicated a heat-stable structure, possibly LOS, in the binding of *H. ducreyi* to HEp-2 cells. Subsequently, Brentjens et al. demonstrated that *H. ducreyi* can adhere to human keratinocytes, cells which would be in contact with *H. ducreyi* early in the infectious process (7). In this study, we have demonstrated that the Tn*916* mutant, defective in LOS biosynthesis, has a markedly reduced ability to adhere to and invade human keratinocytes compared to the parental strain. As described above, this defect in the heptosyltransferase resulted in a truncated LOS structure which lacks the terminal Galβ1-4GlcNAcβ1-3Gal epitope, a structure present on the LOS of 97% of *H. ducreyi* strains as determined by MAb 3F11 binding (9a). This finding implies that this terminal LOS region is involved in attachment and possibly invasion. There is precedence for this finding, as recently reported data implicate LOS (or rough lipopolysaccharide) as an important attachment ligand for other human pathogens (33, 37, 44, 60). Of particular relevance are the data reported by Schwan et al. (44) demonstrating that the terminal portion of the LOS expressed by many strains of *N. gonorrhoeae* is important for attachment and invasion of certain eucaryotic cells. Interestingly, we have previously shown that

the major LOS glycoform of *H. ducreyi* is very similar to a LOS glycoform expressed by most gonococci (29).

While the mechanism(s) of bacterial adherence and invasion of host cells is most certainly a multifactorial event, our data show that the terminal oligosaccharide portion of the LOS is involved in at least one form of attachment to human keratinocytes in vitro. This is a particularly important observation considering that in natural infection, the portal of entry for *H. ducreyi* is most likely a break in the epithelium generated during sexual intercourse (1, 30). Recent studies using an experimental human challenge model of *H. ducreyi* infection have demonstrated that a disruption in the continuity of the cornified layer of the skin is critical for establishment of infection (50). While it is difficult to compare our in vitro data with the actual mechanisms occurring in vivo, it is reasonable to predict that human keratinocytes are likely the first host cells encountered by *H. ducreyi*. Therefore, attachment to these cells may be one of the critical, early steps involved in the pathogenesis of chancroid infections. The results presented in this report implicate the terminal oligosaccharide region of *H. ducreyi* LOS as a bacterial component involved in adherence to, and invasion of, human keratinocytes in vitro. Our data further illustrate that more detailed studies are needed to provide a better understanding of the role of LOS structure as it pertains to *H. ducreyi* infection.

ACKNOWLEDGMENTS

This work was supported by National Institutes of Health grants AI31254 (B.W.G.), AI30006 (A.A.C.), AI24616 (M.A.A.), AI34967 (R.S.M.), and AI38444 (R.S.M.). We also acknowledge support from a grant to R.S.M. from the Children's Hospital Research Foundation as well as support for the UCSF NMR Facility and Mass Spectrometry Facility, the latter of which is supported by the National Center for Research Resources (RR 01614).

We thank Catherine Rebmann, Suzanne van Blerkom, and Corrin Warkentin for excellent technical assistance.

ADDENDUM

While this paper was under review, a report by Stevens et al. was published (51a). This report characterizes the same gene cluster and evaluates the virulence of strains with LOS mutations in the chilled rabbit model.

REFERENCES

1. **Albritton, W. L.** 1989. Biology of *Haemophilus ducreyi*. Microbiol. Rev. **53:**377–389.
2. **Alfa, M. J.** 1992. Cytopathic effect of *Haemophilus ducreyi* for human foreskin cell culture. J. Med. Microbiol. **37:**43–50.
3. **Alfa, M. J., and P. DeGagne.** 1997. Attachment of *Haemophilus ducreyi* to human foreskin fibroblasts involves LOS and fibronectin. Microb. Pathog. **22:**39–46.
4. **Alfa, M. J., P. DeGagne, and P. A. Totten.** 1996. *Haemophilus ducreyi* hemolysin acts as a contact cytotoxin and damages human foreskin fibroblasts in cell culture. Infect. Immun. **64:**2349–2352.
5. **Apicella, M. A., J. M. Griffiss, and H. Schneider.** 1994. Isolation and characterization of lipopolysaccharides, lipooligosaccharides, and lipid A. Methods Enzymol. **235:**242–252.
6. **Auzanneau, F.-I., D. Charon, and L. Szabó.** 1991. Phosphorylated sugars. Part 27. Synthesis and reactions, in acid medium, of 5-O-substituted methyl 3-deoxy-a-D-*manno*-oct-2-ulopyranosidonic acid 4-phosphates. J. Chem. Soc. Perkin Trans. **1:**509–517.
7. **Brentjens, R. J., S. M. Spinola, and A. A. Campagnari.** 1994. *Haemophilus ducreyi* adheres to human keratinocytes. Microb. Pathog. **16:**243–247.
8. **Campagnari, A. A., R. Karalus, M. Apicella, W. Melaugh, A. J. Lesse, and B. W. Gibson.** 1994. Use of pyocin to select a *Haemophilus ducreyi* variant defective in lipooligosaccharide biosynthesis. Infect. Immun. **62:**2379–2386.
9. **Campagnari, A. A., L. M. Wild, G. E. Griffiths, R. J. Karalus, M. A. Wirth, and S. M. Spinola.** 1991. Role of lipooligosaccharides in experimental dermal lesions caused by *Haemophilus ducreyi*. Infect. Immun. **59:**2601–2608.

9a. **Campagnari, A. A.** Unpublished data.

10. **Clark-Curtiss, J. E., W. R. Jacobs, M. A. Docherty, L. R. Ritchie, and R. Curtiss III.** 1985. Molecular analysis of DNA and construction of genomic libraries of *Mycobacterium leprae*. J. Bacteriol. **161:**1093–1102.
11. **Cope, L. D., S. Lumbley, J. L. Latimer, J. Klesney-Tait, M. K. Stevens, L. S. Johnson, M. Purven, R. S. Munson, Jr., T. Lagergard, J. D. Radolf, and E. J. Hansen.** 1997. A diffusible cytotoxin of *Haemophilus ducreyi*. Proc. Natl. Acad. of Sci. USA **94:**4050–4061.

11a. **Gibson, B.** Unpublished data.

12. **Gibson, B. W., J. J. Engstrom, C. M. John, W. Hines, and A. M. Falick.** 1997. Characterization of bacterial lipooligosaccharides by delayed extraction matrix-assisted laser ionization time-of-flight mass spectrometry. J. Am. Soc. Mass Spectrom. **8:**645–658.
13. **Gibson, B. W., W. Melaugh, N. J. Phillips, M. A. Apicella, A. A. Campagnari, and J. M. Griffiss.** 1993. Investigation of the structural heterogeneity of lipooligosaccharides from pathogenic *Haemophilus* and *Neisseria* species and of R-type lipopolysaccharides from *Salmonella typhimurium* by electrospray mass spectrometry. J. Bacteriol. **175:**2702–2712.
14. **Helander, I. M., I. Kilpelainen, and M. Vaara.** 1994. Increased substitution of phosphate groups in lipopolysaccharides and lipid A of the polymyxin-resistant *pmrA* mutants of *Salmonella typhimurium*: a 31P-NMR study. Mol. Microbiol. **11:**481–487.
15. **High, N. J., M. E. Deadman, and E. R. Moxon.** 1993. The role of a repetitive DNA motif (5′-CAAT-3′) in the variable expression of the *Haemophilus influenzae* lipopolysaccharide epitope alpha Gal(1-4)beta Gal. Mol. Microbiol. **9:**1275–1282.
16. **Jessamine, P. G., and A. R. Ronald.** 1990. Chancroid and the role of genital ulcer disease in the spread of human retroviruses. Med. Clin. North Am. **74:**1417–1431.
17. **Kelly, J., H. Masoud, M. B. Perry, J. C. Richards, and P. Thibault.** 1996. Separation and characterization of O-deacylated lipooligosaccharides and glycans derived from *Moraxella catarrhalis* using capillary electrophoresis-electrospray mass spectrometry and tandem mass spectrometry. Anal. Biochem. **233:**15–30.
18. **Klena, J. D., E. Pradel, and C. A. Schnaitman.** 1992. Comparison of lipopolysaccharide biosynthesis genes *rfaK*, *rfaL*, *rfaY*, and *rfaZ* of *Escherichia coli* K-12 and *Salmonella typhimurium*. J. Bacteriol. **174:**4746–4752.
19. **Kreiss, J. K., R. Coombs, F. Plummer, K. K. Holmes, B. Nikora, W. Cameron, E. Ngugi, J. O. Ndinya Achola, and L. Corey.** 1989. Isolation of human immunodeficiency virus from genital ulcers in Nairobi prostitutes. J. Infect. Dis. **160:**380–384.
20. **Kulshin, V. A., U. Zahringer, B. Lindner, C. E. Frasch, C. M. Tsai, B. A. Dmitriev, and E. T. Rietschel.** 1992. Structural characterization of the lipid A component of pathogenic *Neisseria meningitidis*. J. Bacteriol. **174:**1793–1800.
21. **Lagergard, T.** 1992. The role of *Haemophilus ducreyi* bacteria, cytotoxin, endotoxin and antibodies in animal models for study of chancroid. Microb. Pathog. **13:**203–217.
22. **Lagergard, T., M. Purven, and A. Frisk.** 1993. Evidence of *Haemophilus ducreyi* adherence to and cytotoxin destruction of human epithelial cells. Microb. Pathog. **14:**417–431.
23. **Levery, S. B., and S. Hakomori.** 1987. Microscale methylation analysis of glycolipids using capillary gas chromatography-chemical ionization mass fragmentography with selected ion monitoring. Methods Enzymol. **138:**13–25.
24. **Maniatis, T., E. F. Fritsch, and J. Sambrook.** 1982. Molecular cloning: a laboratory manual. Cold Spring Harbor Laboratory, Cold Spring Harbor, N.Y.
25. **Masoud, H., E. R. Moxon, A. Martin, D. Krajcarski, and J. C. Richards.** 1997. Structure of the variable and conserved lipopolysaccharide oligosaccharide epitopes expressed by *Haemophilus influenzae* serotype b strain Eagan. Biochemistry **36:**2091–2103.
26. **Masoud, H., M. B. Perry, and J. C. Richards.** 1994. Characterization of the lipopolysaccharide of *Moraxella catarrhalis*. Structural analysis of the lipid A from *M. catarrhalis* serotype A lipopolysaccharide. Eur. J. Biochem. **220:**209–216.
27. **Melaugh, W., A. A. Campagnari, and B. W. Gibson.** 1996. The lipooligosaccharides of *Haemophilus ducreyi* are highly sialylated. J. Bacteriol. **178:**564–570.
28. **Melaugh, W., N. J. Phillips, A. A. Campagnari, R. Karalus, and B. W. Gibson.** 1992. Partial characterization of the major lipooligosaccharide from a strain of *Haemophilus ducreyi*, the causative agent of chancroid, a genital ulcer disease. J. Biol. Chem. **267:**13434–13439.
29. **Melaugh, W., N. J. Phillips, A. A. Campagnari, M. V. Tullius, and B. W. Gibson.** 1994. Structure of the major oligosaccharide from the lipooligosaccharide of Haemophilus ducreyi strain 35000 and evidence for additional glycoforms. Biochemistry **33:**13070–13078.
30. **Morse, S. A.** 1989. Chancroid and *Haemophilus ducreyi*. Clin. Microbiol. Rev. **2:**137–157.
31. **Palmer, K. L., W. E. Goldman, and R. S. Munson, Jr.** 1996. An isogenic haemolysin-deficient mutant of *Haemophilus ducreyi* lacks the ability to produce cytopathic effects on human foreskin fibroblasts. Mol. Microbiol. **21:**13–19.

32. **Palmer, K. L., and R. S. Munson, Jr.** 1995. Cloning and characterization of the genes encoding the hemolysin of *Haemophilus ducreyi*. Mol. Microbiol. **18:**821–830.
33. **Paradis, S.-E., D. Dubreuil, S. Rioux, M. Gottschalk, and M. Jacques.** 1994. High-molecular-mass lipopolysaccharides are involved in *Actinobacillus pleuropneumoniae* adherence to porcine respiratory tract cells. Infect. Immun. **62:**3311–3319.
34. **Phillips, N. J., M. A. Apicella, J. M. Griffiss, and B. W. Gibson.** 1992. Structural characterization of the cell surface lipooligosaccharides from a nontypable strain of *Haemophilus influenzae*. Biochemistry **31:**4515–4526.
35. **Phillips, N. J., M. A. Apicella, J. M. Griffiss, and B. W. Gibson.** 1993. Structural studies of the lipooligosaccharides from *Haemophilus influenzae* type b strain A2. Biochemistry **32:**2003–2012.
36. **Phillips, N. J., C. M. John, L. G. Reinders, B. W. Gibson, M. A. Apicella, and J. M. Griffiss.** 1990. Structural models for the cell surface lipooligosaccharides of *Neisseria gonorrhoeae* and *Haemophilus influenzae*. Biomed. Environ. Mass Spectrom. **19:**731–745.
37. **Pier, G., M. Grout, T. Zaidi, J. Olsen, L. Johnson, J. Yankaskas, and J. Goldberg.** 1996. Role of mutant CFTR in hypersusceptibility of cystic fibrosis patients to lung infections. Science **271:**64–67.
38. **Potter, M. D., and R. Y. Lo.** 1995. Cloning and characterization of a gene from *Pasteurella haemolytica* A1 involved in lipopolysaccharide biosynthesis. FEMS Microbiol. Lett. **129:**75–81.
39. **Preston, A., R. E. Mandrell, B. W. Gibson, and M. A. Apicella.** 1996. The lipooligosaccharides of pathogenic gram-negative bacteria. Crit. Rev. Microbiol. **22:**139–180.
40. **Purven, M., and T. Lagergard.** 1992. *Haemophilus ducreyi*, a cytotoxin-producing bacterium. Infect. Immun. **60:**1156–1162.
41. **Rick, P. D.** 1987. Lipopolysaccharide biosynthesis, p. 648–662. *In* F. C. Neidhardt, J. L. Ingraham, K. B. Low, B. Magasanik, M. Schaechter, and H. E. Umbarger (ed.), *Escherichia coli* and *Salmonella typhimurium*: cellular and molecular biology, vol. 1. American Society for Microbiology, Washington, D.C.
42. **Roland, K. L., L. E. Martin, C. R. Esther, and J. K. Spitznagel.** 1993. Spontaneous *pmrA* mutants of *Salmonella typhimurium* LT2 define a new two-component regulatory system with a possible role in virulence. J. Bacteriol. **175:**4154–4164.
43. **Ronald, A. R., and F. A. Plummer.** 1985. Chancroid and *Haemophilus ducreyi*. Ann. Intern. Med. **102:**705–707.
44. **Schwan, E. T., B. D. Robertson, H. Brade, and J. P. M. van Putten.** 1995. Gonococcal *rfaF* mutants express Rd2 chemotype LPS and do not enter epithelial host cells. Mol. Microbiol. **15:**267–275.
45. **Schweda, E. K., J. A. Jonasson, and P. E. Jansson.** 1995. Structural studies of lipooligosaccharides from *Haemophilus ducreyi* ITM 5535, ITM 3147, and a fresh clinical isolate, ACY1: evidence for intrastrain heterogeneity with the production of mutually exclusive sialylated or elongated glycoforms. J. Bacteriol. **177:**5316–5321.
46. **Schweda, E. K., A. C. Sundstrom, L. M. Eriksson, J. A. Jonasson, and A. A. Lindberg.** 1994. Structural studies of the cell envelope lipopolysaccharides from *Haemophilus ducreyi* strains ITM 2665 and ITM 4747. J. Biol. Chem. **269:**12040–12048.
47. **Scott, J. R.** 1992. Sex and the single circle: conjugative transposition. J. Bacteriol. **174:**6005–6010.
48. **Silhavy, T., M. L. Berman, and L. W. Enquist.** 1984. Experiments with gene fusions. Cold Spring Harbor Laboratory, Cold Spring Harbor, N.Y.
49. **Spinola, S. M., T. J. Hiltke, K. Fortney, and K. L. Shanks.** 1996. The conserved 18,000-molecular-weight outer membrane protein of *Haemophilus ducreyi* has homology to PAL. Infect. Immun. **64:**1950–1955.
50. **Spinola, S. M., L. M. Wild, M. A. Apicella, A. A. Gaspari, and A. A. Campagnari.** 1994. Experimental human infection with *Haemophilus ducreyi*. J. Infect. Dis. **169:**1146–1150.
51. **Stevens, M. K., L. D. Cope, J. D. Radolf, and E. J. Hansen.** 1995. A system for generalized mutagenesis of *Haemophilus ducreyi*. Infect. Immun. **63:** 2976–2982.

51a. **Stevens, M. K., J. Klesney-Tait, S. Lumbley, K. A. Walters, A. M. Joffe, J. D. Radolf, and E. J. Hansen.** 1997. Identification of tandem genes involved in lipooligosaccharide expression by *Haemophilus ducreyi*. Infect. Immun. **65:** 651–660.

52. **St. Geme III, J. W., and S. Falkow.** 1990. *Haemophilus influenzae* adheres to and enters cultured human epithelial cells. Infect. Immun. **58:**4036–4044.
53. **Telzak, E. E., M. A. Chiasson, P. J. Bevier, R. L. Stoneburner, K. G. Castro, and H. W. Jaffe.** 1993. HIV-1 seroconversion in patients with and without genital ulcer disease. Ann. Intern. Med. **119:**1181–1186.
54. **Totten, P. A., D. V. Norn, and W. E. Stamm.** 1995. Characterization of the hemolytic activity of *Haemophilus ducreyi*. Infect. Immun. **63:**4409–4416.
55. **Tuffrey, M., F. Alexander, R. C. Ballard, and D. Taylor-Robinson.** 1990. Characterization of skin lesions in mice following intradermal inoculation of *Haemophilus ducreyi*. J. Exp. Pathol. **71:**233–244.
56. **Vestal, M. L., P. Juhasz, and S. A. Martin.** 1995. Delayed extraction matrix-assisted laser desorption time-of flight mass spectrometry. Rapid Commun. Mass Spectrom. **9:**1044–1050.
57. **Wang, R. F., and S. R. Kushner.** 1991. Construction of versatile low-copy-number vectors for cloning, sequencing and gene expression in *Escherichia coli*. Gene **100:**195–199.
58. **Wasserheit, J. N.** 1992. Epidemiological synergy. Interrelationships between human immunodeficiency virus infection and other sexually transmitted diseases. Sex. Transm. Dis. **19:**61–77.
59. **Willson, P. J., W. L. Albritton, L. Slaney, and J. K. Setlow.** 1989. Characterization of a multiple antibiotic resistance plasmid from *Haemophilus ducreyi*. Antimicrob. Agents Chemother. **33:**1627–1630.
60. **Zaidi, T., S. Fleiszig, M. Preston, J. Goldberg, and G. Pier.** 1996. Lipopolysaccharide outer core is a ligand for corneal cell binding and ingestion of *Pseudomonas aeruginosa*. Invest. Ophthalmol. Visual Sci. **37:**976–986.